Tunneling splitting in double-proton transfer: Direct diagonalization results for porphycene

Zorka Smedarchina, Willem Siebrand, and Antonio Fernández-Ramos

Citation: The Journal of Chemical Physics **141**, 174312 (2014); doi: 10.1063/1.4900717
View online: http://dx.doi.org/10.1063/1.4900717
View Table of Contents: http://scitation.aip.org/content/aip/journal/jcp/141/17?ver=pdfcov
Published by the AIP Publishing

Tunneling splitting in double-proton transfer: Direct diagonalization results for porphycene

Zorka Smedarchina,[1] Willem Siebrand,[1] and Antonio Fernández-Ramos[2,a)]
[1]*Steacie Institute for Molecular Sciences, National Research Council of Canada, Ottawa, Ontario K1A 0R6, Canada*
[2]*Department of Physical Chemistry and Center for Research in Biological Chemistry and Molecular Materials, University of Santiago de Compostela, 15706 Santiago de Compostela, Spain*

(Received 29 July 2014; accepted 19 October 2014; published online 5 November 2014)

Zero-point and excited level splittings due to double-proton tunneling are calculated for porphycene and the results are compared with experiment. The calculation makes use of a multidimensional imaginary-mode Hamiltonian, diagonalized directly by an effective reduction of its dimensionality. Porphycene has a complex potential energy surface with nine stationary configurations that allow a variety of tunneling paths, many of which include classically accessible regions. A symmetry-based approach is used to show that the zero-point level, although located above the *cis* minimum, corresponds to concerted tunneling along a direct *trans* − *trans* path; a corresponding *cis* − *cis* path is predicted at higher energy. This supports the conclusion of a previous paper [Z. Smedarchina, W. Siebrand, and A. Fernández-Ramos, J. Chem. Phys. **127**, 174513 (2007)] based on the instanton approach to a model Hamiltonian of correlated double-proton transfer. A multidimensional tunneling Hamiltonian is then generated, based on a double-minimum potential along the coordinate of concerted proton motion, which is newly evaluated at the RI-CC2/cc-pVTZ level of theory. To make it suitable for diagonalization, its dimensionality is reduced by treating fast weakly coupled modes in the adiabatic approximation. This results in a coordinate-dependent mass of tunneling, which is included in a unique Hermitian form into the kinetic energy operator. The reduced Hamiltonian contains three symmetric and one antisymmetric mode coupled to the tunneling mode and is diagonalized by a modified Jacobi-Davidson algorithm implemented in the Jadamilu software for sparse matrices. The results are in satisfactory agreement with the observed splitting of the zero-point level and several vibrational fundamentals after a partial reassignment, imposed by recently derived selection rules. They also agree well with instanton calculations based on the same Hamiltonian.
 [http://dx.doi.org/10.1063/1.4900717]

I. INTRODUCTION

In many chemical and biological systems subject to proton transfer, the protons move in pairs along hydrogen bonds weak enough to provide a barrier. At low temperatures this motion takes the form of tunneling through this barrier. To calculate transfer rates and level splittings resulting from any tunneling process, we need a method that can effectively reduce the dimensionality of the tunneling Hamiltonian, by separating the tunneling modes, which move in a double-minimum potential, from the harmonic modes coupled to it. For single-proton transfer this leads to a one-dimensional (1D) effective Hamiltonian that can be handled by well-known methods, but for double-proton transfer, it leads to a 2D effective Hamiltonian that can engender multiple tunneling paths. It turns out, however, that for many of the molecules in which double-proton transfer has been observed, this transfer can be handled by 1D methods because the protons either move independently or concertedly as a pair. Independent motion occurs, e.g., in porphine, where there is a sufficiently stable intermediate state, leading to step-wise transfer, whereas concerted transfer occurs, e.g., in the formic acid dimer, where there is no such state.[1] In both of these species the protons move along two identical bonds, but in the complex 2-pyridone-2-hydroxypyridine, they move concertedly along hydrogen bonds that are different and of unequal strength.[2] Thus far little attention has been paid to cases where an intermediate state of low stability plays a part, an example being porphycene, the subject of the present investigation.

Based on the realization that it would be useful to have a method that can deal with double-proton tunneling irrespective of the strength of the correlation between the two proton motions, we developed in a previous paper,[3] hereafter referred to as CDPT, a molecular model for this purpose. Recently, McKenzie[4] has developed a model for double proton transfer based on diabatic states, which leads to four different classes of ground state potential energy surfaces (PES), three of them being the same as the ones described in Refs. 1 and 3, and a new type with just one minimum and no transition state. The CDPT model consists of two identical interacting hydrogen bonds to provide a general description of the dynamics of correlated double-proton transfer that is valid for concerted as well as stepwise transfer and for any situation in between. Using this model, we found by the quasiclassical instanton approach, that the zero-point tunneling splitting, which is defined by the Euclidean action at zero temperature

a)Electronic mail: qf.ramos@usc.es

($T = 0$), is always due to concerted double-proton transfer, the tunneling probability at $T = 0$ being highest when the protons move together as long as they are correlated. This implies that in molecules with a stable intermediate any observed zero-point tunneling splitting is due to concerted tunneling, independent of the energy of the intermediate. This important corollary, which is anti-intuitive, deserves an experimental test. It is the purpose of this contribution to provide such a test. To this end we calculate tunneling splittings for the molecule porphycene,[5] a porphyrin isomer, for which such splittings have been measured recently, not only of the zero-point level but also of several vibrationally excited levels.[6–8] In porphycene two hydrogens are bound to an inner ring of the four nitrogens, which form a rectangle and are thus pairwise equivalent. Calculations[9–12] show that in the equilibrium configuration they are oscillating between the two equivalent *trans* positions, to be denoted by MIN. The *cis* configuration (INT), with both hydrogens on a pair of adjacent nitrogens with the larger separation, has an energy higher than the *trans* configuration. The *cis* and *trans* configurations are separated by a first-order saddle point (TS); there are four such barriers. Finally, the two *trans* and the two *cis* configurations are each separated by a single second-order saddle point that forms an absolute maximum (MAX). Altogether, a PES of this type has nine stationary configurations, illustrated in Fig. 1 for porphycene, which allows a multitude of tunneling paths, as detailed in CDPT and in Sec. IV.

Waluk and coworkers[6–8] have measured the tunneling splitting for the zero-point level and several modes assigned as totally symmetric and combinations thereof in emission spectra, both in cold beams and in helium droplets; they have also tried to measure the splitting for the zero-point level of porphycene-d_1, which turned out to be below the level of resolution (about 1 cm^{-1}), but was estimated to be about 0.6 cm^{-1} on the basis of the observed splitting of an excited level. The observed zero-point splitting of 4.43 cm^{-1} in porphycene-d_0 was roughly equal to that observed for two of the excited levels assigned to totally symmetric modes, while two other modes, also assigned as totally symmetric, showed no resolvable splitting; bands associated with the N···N stretching mode of the hydrogen bond showed a splitting of about 12 cm^{-1} in porphycene-d_0 and 2.3 cm^{-1} in porphycene-d_1. The authors tentatively associated the observed decrease and increase relative to the zero-point splitting to changes in the tunneling distance. These observations may seem to contradict recently reported selection rules,[13] which assert that excitation of symmetric modes will generally increase the splitting for vibrations interacting with the tunneling mode, but it should be remembered that these selection rules apply to the symmetries of the modes in the transition state rather than in the equilibrium configuration.

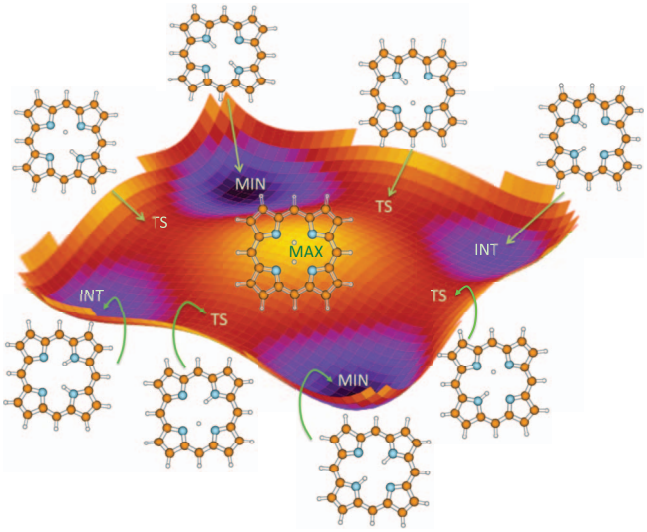

FIG. 1. Schematic three-dimensional potential energy surface appropriate to double-proton transfer in porphycene, where MIN corresponds to the *trans* and INT to the *cis* configuration. TS and MAX indicates first- and second-order saddle point, respectively.

In a series of papers we have calculated tunneling splittings starting from a multidimensional (MD) Hamiltonian centered at the point of highest symmetry of the PES, namely the top of the barrier separating the two equivalent equilibrium configurations, which allows us to make full use of the symmetry of the system and to apply these selection rules; extended discussion and references to the original work can be found in our earlier papers.[13–15] This implies that the tunneling mode will have an imaginary frequency at this point. Since in porphycene there are two transferring protons, the point of highest symmetry is a second-order saddle point, with two imaginary modes, one corresponding to *trans–trans* and the other to *cis–cis* transitions. In CDPT we showed that, in the quasiclassical approximation, the zero-point splitting of a pair of correlated hydrogen bonds will be governed by concerted transfer between the lowest minima, which in porphycene are the *trans* configurations. In Sec. II we rederive this conclusion on the basis of symmetry arguments without using this approximation, and extend it to the splitting of higher levels. In the Appendix, we support it with numerical calculations based on direct diagonalization of a 2D model Hamiltonian.

Based on this conclusion, we generate the imaginary-mode MD Hamiltonian for concerted tunneling, which is newly derived from the structure and Hessians calculated at the RI-CC2/cc-pVTZ level of theory.[16,17] To solve this Hamiltonian, which consists of a double-minimum potential along the concerted tunneling path coupled to a number of skeletal vibrations, we use a new method of direct diagonalization.[18] The generation of the PES at RI-CC2/cc-pVTZ level of theory is discussed in Sec. III and the diagonalization results are reported in Sec. IV. We recently showed[18] that such a Hamiltonian can be diagonalized if the number of coupled vibrations is kept within certain limits. This we achieve in two ways: first by restricting, as before, coupling between tunneling and skeletal modes to terms linear in the skeletal modes, which eliminates all modes that are neither symmetric nor antisymmetric to the dividing plane of the transfer reaction; and second, by treating modes that are fast on the time scale of tunneling in the adiabatic approximation.[19,20] The latter approximation renders the mass of the tunneling pair of protons dependent on the tunneling coordinate, so that this coordinate enters the expression for the kinetic energy operator. A unique Hermitian form for this operator was constructed and tested in Ref. 18. The diagonalization procedure

is carried out by a modified Jacobi-Davidson algorithm implemented in the Jadamilu software for sparse matrices.[21] In Sec. V we compare observed and calculated tunneling splittings for the zero-point level and several fundamental levels. We report also tunneling splittings obtained with the approximate instanton method as implemented in the DOIT code (AIM/DOIT approach), used previously,[22,23] which employs a MD Hamiltonian for concerted tunneling that includes all the (linearly) coupled modes. Since both calculations use the same quantum-chemical input data, this allows comparison of the accuracy of the two methods.

II. SYMMETRY AND THE MECHANISM OF DOUBLE PROTON TRANSFER

In a symmetric molecule with a single hydrogen bond, such as malonaldehyde, the zero-point level is split into two levels when the proton can tunnel through the barrier separating the two equivalent equilibrium configurations. In molecules with two equivalent symmetric hydrogen bonds, the zero-point level should therefore be split into four levels. If there is no interaction between the two hydrogen bonds, these levels should be pairwise degenerate, the problem being reduced to that of a single hydrogen bond, but since hydrogen bonds are polar, this degeneracy tends to be lifted in actual molecules. The resulting fourfold splitting can thus be traced back to two causes, tunneling through a barrier and interaction between the tunneling protons. If tunneling dominates, each tunneling level will be split into two components due to the interaction, and if the interaction dominates, there will be two stable configurations of different energy, each split into two components due to single-particle tunneling, the single particle being a concertedly moving pair of protons. When the two hydrogen bonds are parallel, as in the CDPT model and in porphycene, the two configurations may be identified as *cis* and *trans*.

In most molecules and complexes studied to date the electrostatic interaction between the two protons, roughly measured by the calculated *cis–trans* energy difference, is much larger than the tunneling interaction, roughly measured by the observed tunneling splitting. A typical example is the formic acid dimer in which the *cis* configuration is unstable and leads to decomposition of the dimer. Its observed tunneling splitting is thus readily assigned to concerted transfer of a pair of protons in the *trans* configuration. In porphycene the hydrogen bonds are farther apart and weaker, leading to a stable *cis* configuration, but the calculated *cis* − *trans* energy difference of about 760 cm^{-1}, as given in Sec. III, is still much larger than the observed tunneling splitting of 4.4 cm^{-1}; therefore the zero-point splitting should again be assigned to concerted transfer of a pair of protons in the *trans* configuration. The situation retains some ambiguity, however, since the tunneling splitting relevant to the comparison is that for single-proton transfer with half the mass of the proton pair. Also, zero-point energy differences may affect the potentials and one may expect split levels due to tunneling in the *cis* configuration, which have not been observed.

Using point group symmetry, we note that the configuration of the second-order saddle point (MAX) belongs to point group D_{2h}, while that of the *trans* configuration (MIN) belongs to C_{2h}, and that of the *cis* configuration (INT) to C_{2v}. The two modes with imaginary frequency (tunneling modes) are antisymmetric with respect to the plane perpendicular to the molecule that contains both hydrogen atoms, as shown in Fig. 2. This assigns the *trans* antisymmetric mode to the representation b_{3g} and the *cis* antisymmetric mode to the representation b_{2u} in D_{2h}. Both modes correspond to concerted double-proton transfer and lead to the totally symmetric representations a_g and a_1 of MIN and INT, respectively. Their splittings can be calculated by standard single-particle tunneling methods and should be observable if the proper tools are available. It may happen that the level splitting in INT approaches the vibrational spacing of the b_{2u} mode, but this would not detract from the present interpretation. If a molecule can be found in which the *cis–trans* energy difference roughly matches the tunneling interaction, the CDPT model still would apply but the splitting might no longer be interpretable in terms of single-particle tunneling.

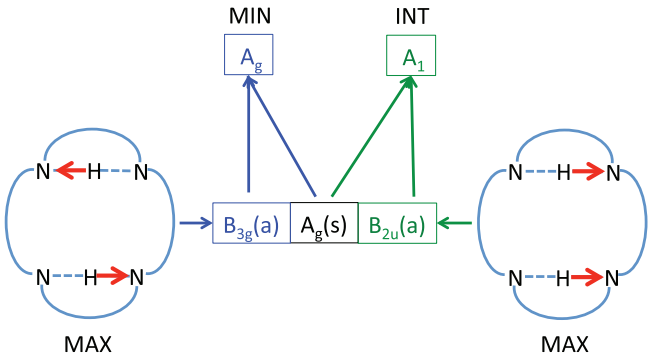

FIG. 2. Scheme depicting the two antisymmetric (a) tunneling modes at MAX, as well as their character representation in the D_{2h} point group symmetry. Those modes lead to the totally symmetric a_g and a_1 representations in MIN and INT, respectively. It also indicates that the linearly displaced symmetric modes (s) correspond to totally symmetric representations in all configurations.

These symmetry arguments are very general and remain valid in the presence of normal modes weakly coupled to the tunneling modes. Given the symmetries of the stationary states and the dominance of the proton-proton coupling over the tunneling interaction, the *cis–cis* and *trans–trans* tunnelings are separable and will each follow a concerted path through the barrier represented by the second-order saddle point. This result confirms the earlier conclusions derived from instanton calculations. It will be further illustrated by model calculations in the Appendix.

III. POTENTIAL ENERGY SURFACE OF PORPHYCENE

As mentioned in the Introduction, porphycene is a molecule in which two equivalent protons move between four minima in the PES, two equivalent *trans* and two equivalent *cis* positions. High-level quantum-chemical calculations[6–9] indicate that these two minima are close in energy, with the *trans* configuration the more stable, leading to a complex PES for the proton motion as illustrated in Fig. 1. It is thus an ideal molecule to probe whether the theoretical approach based on

the imaginary-mode Hamiltonian can deal with double-proton tunneling splittings in a molecule of unusual complexity.

To obtain accurate input data for the calculation of tunneling splittings in porphycene-d_0, -d_1, and -d_2, we have carried out geometry optimizations and Hessian calculations for the stationary points at the RI-CC2/cc-pVTZ level of theory [second-order approximated coupled-cluster model with the resolution-of-identity approximation (RI-CC2)[16] and cc-pVTZ basis set[17]]. It has been shown that, for electron-rich compounds in particular, as in the present case, RI-CC2 outperforms MP2.[24] An alternative to the RI-CC2 calculations performed in this work, based also on coupled cluster and designed for large molecules, would be the orbital-specific-virtual local coupled cluster singles and doubles (OSV-LCCSD) method.[25] The relevant structural and energetic parameters are summarized in Fig. 3 and compared with previous calculations carried out in Ref. 12. As seen from this figure, at RI-CC2/cc-pVTZ level the INT, TS, and MAX configurations are higher by 2.18 kcal/mol, 2.93 kcal/mol, and 4.08 kcal/mol, respectively, than the MIN configuration. The figure also illustrates that the structural parameters of the hydrogen bond network for MAX, calculated at this level of theory are quite similar to those obtained at the B3LYP/6-31+G(d,p) level, unlike those of MIN, where the RI-CC2 level leads to a tighter structure and therefore to lower barriers when compared to the B3LYP electronic structure method. It

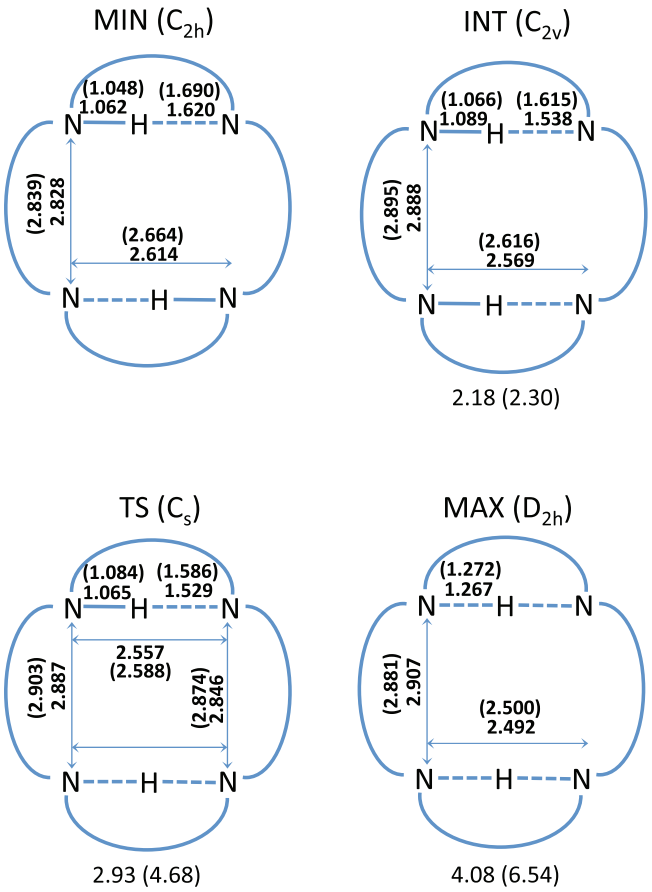

FIG. 3. Hydrogen bond network distances (in Å) and relative energies (in kcal/mol below each structure) of the stationary points of porphycene calculated at the RI-CC2/cc-pVTZ and B3LYP/6-31+G(d) (in parentheses) levels.

should be noticed that some functionals, including B3LYP, tend to underestimate the strength of the hydrogen bonds, leading to hydrogen transfer barriers which are too high.[26] A very recent work also points out that a good description of the network of hydrogen bonds of water by Density Functional Theory methods needs to include exact exchange and dispersion corrections,[27] while B3LYP includes only the former correction. [Note that the calculations based on the PES at B3LYP/6-31+G(d,p) level carried out when Ref. 12 was published, yield zero-point tunneling splittings that are about an order of magnitude smaller than the observed values. This was probably due to an overestimation of the barrier height by the B3LYP calculations.] In the present study the RI-CC2 calculations were carried out with the TURBOMOLE package.[28] The calculated frequencies of the normal modes of the stationary points of porphycene are summarized in the supplementary material.[29] The parameters relevant to the generation of the imaginary-mode Hamiltonian, based on the Hessians, are reported in Sec. IV for the three isotopes porphycene-d_0, -d_1, and -d_2.

The calculated PES shows nine stationary points belonging to four configurations MIN, MAX, INT, and TS. In the simplest approach, this complex PES can be represented by the 2D model introduced in CDPT, where two correlated protons are best described in terms of the collective proton coordinates $x_{s,a} = (x_1 \pm x_2)/2$ and mass $m_s = m_1 + m_2$, rather than individual-particle parameters $x_{1,2}$ and $m_{1,2}$, respectively; this model is discussed in detail in the Appendix. It exhibits the four categories of stationary points and is defined by three parameters, one of which is the proton-proton correlation parameter G. Following the analysis in CDPT, we evaluate the proton-proton correlation parameter in porphycene from the curvatures at MAX along these coordinates; we obtain a value $G = 0.19$, which means that we are dealing with correlation much stronger than in porphine (which is similar to porphycene but without the inner hydrogen bonds) treated in CDPT as an example, for which $G = 0.06$. The relation of this stronger correlation to the transfer mechanism and thus to the observed tunneling splittings is detailed in Sec. IV.

As indicated in Sec. II, in the tautomerization process the two protons oscillate between the two equivalent *trans* positions; these structures belong to the C_{2h} point group. Along the short side of the rectangle the spacing is much closer than that in porphine leading to substantial hydrogen bonding. The distance of 2.614 Å between the donor and the acceptor in the *trans* structure indicates a regime close to the so-called low-barrier hydrogen bonds.[30,31] Along the long side the spacing is slightly smaller than in porphine, but the proton transfer distance is considerably longer since the proton is drawn towards the hydrogen bond along the short side. Hence one expects the double-proton transfer to be essentially confined to the hydrogen bonded pair of nitrogens and to be considerably more rapid than in porphine. The *cis* configuration, with both hydrogens on a pair of adjacent nitrogens with the larger separation, has an energy slightly higher than the *trans* configuration and belongs to the C_{2v} point group. The transition state between the two *trans* configurations is the same as that between the two *cis* configurations, implying that it is a second-order saddle point, which belongs to the D_{2h} point group. Since the

alternative *cis* configuration, with both hydrogens on a pair of adjacent nitrogens with the smaller separation, breaks the hydrogen bond and leads to strong repulsion between the hydrogens, it is not expected to play a part in the transfer.

IV. DIAGONALIZATION OF THE HAMILTONIAN OF CONCERTED TUNNELING WITH POSITION-DEPENDENT MASS

The symmetry arguments presented in Sec. II show that the zero-point tunneling splitting in porphycene is due to concerted double-proton tunneling between the two *trans* configuration through MAX. This conclusion is confirmed in the Appendix by numerical calculations on the model 2D Hamiltonian of two correlated protons, generated from the porphycene data of Sec. III. The results of these calculations are illustrated in Fig. 4, which shows the wave functions of the six lowest eigenstates. Specifically, it shows that the wave functions of the ground-state doublet $\phi_0^{+/-}$, depicted in the first row, are localized in the *trans* configuration and have the typical behavior of 1D concerted tunneling *trans*-MAX-*trans* as predicted by symmetry. On this basis we now proceed

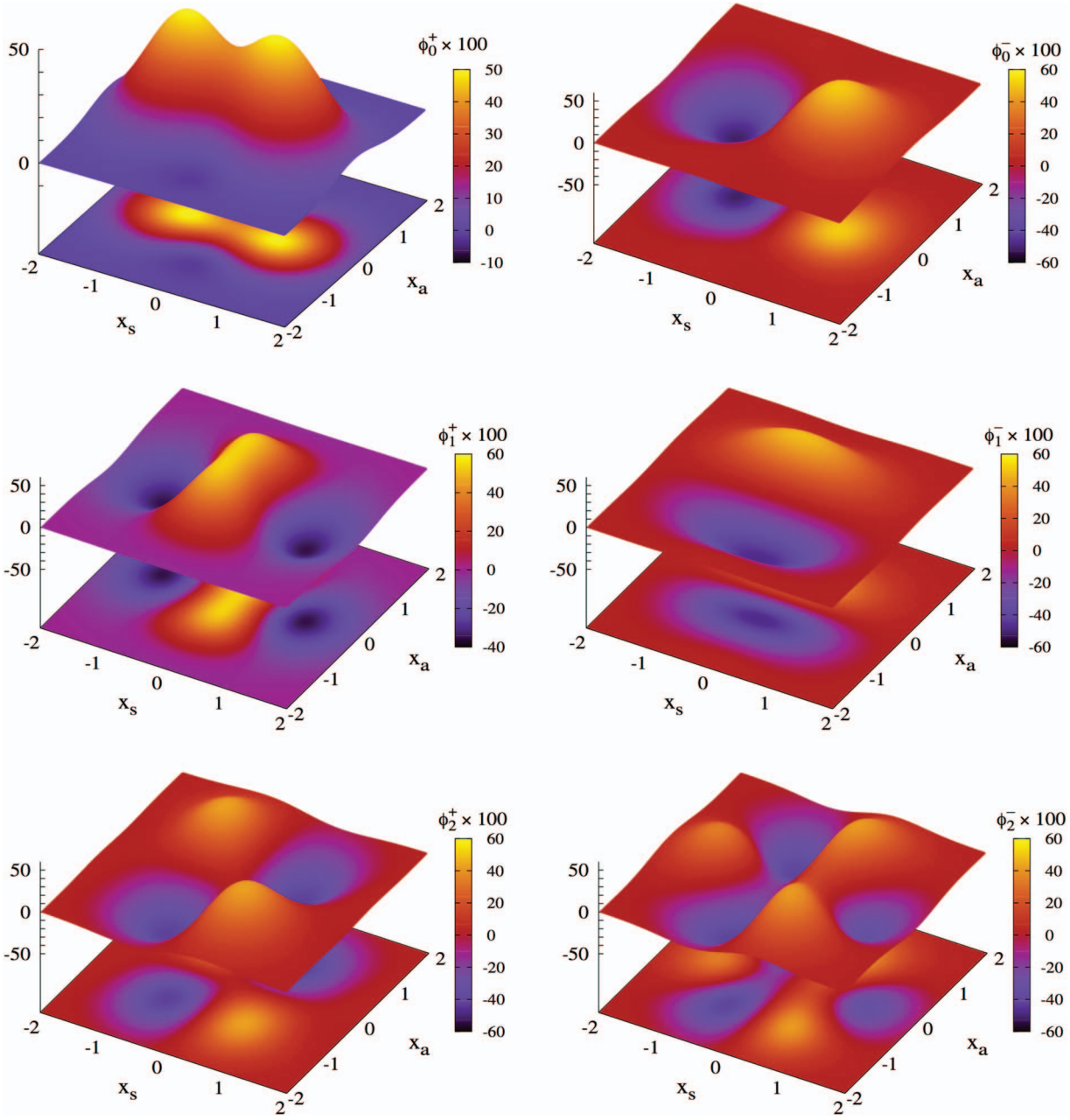

FIG. 4. Wave functions (WFs) of the six lowest eigenstates, obtained numerically for the 2D model Hamiltonian of Eq. (A3), whose stationary points MIN; INT; TS; and MAX are at 0, 800; 980; and 1440 cm^{-1}, respectively. The eigenstates with energies below MAX form doublets: $E_0^{+/-} = 989.3/1024.6\ cm^{-1}$ and $E_1^{+/-} = 1453.4/1493.5\ cm^{-1}$, whose WFs $\phi_0^{+/-}$ and $\phi_1^{+/-}$ are depicted in the 1st and 2nd row, respectively. Note that, despite the fact that $E_0 >$ INT, $\phi_0^{+/-}$ are localized at MIN and have the typical character of 1D concerted tunneling *trans*-MAX-*trans* as predicted by symmetry. Similarly, $E_1 \geq$ MAX, but the wave functions $\phi_1^{+/-}$ retain the image of concerted tunneling *cis*-MAX-*cis* as again predicted by symmetry. The last row shows WFs of decoupled protons which correspond to the next two levels $E_2^{+/-} = 2442.9/3255.6\ cm^{-1}$, situated well above MAX.

by deriving a MD Hamiltonian where $x_{cis} \equiv 0$, that includes all skeletal modes coupled to the 1D two-particle tunneling mode $x \equiv x_{trans}$, and use MAX as the origin of the vibrational coordinates. In CDPT and in the Appendix, including Fig. 4, we use the notation x_a for x_{cis} and x_s for x_{trans}, where a and s are symmetry labels, not to be confused with the labels a and s used as running numbers for harmonic normal modes that are, respectively, antisymmetric and symmetric with respect to the dividing plane $x = 0$. Our procedure will be the same as that used to derive the MD imaginary-mode Hamiltonian (iMDH for short) applied previously to instanton calculations, most recently discussed in Refs. 14 and 15.

To account for the observed splittings, we diagonalize this iMDH in the manner we described recently.[18] We use mass-weighted normal modes x for the tunneling mode and y_j for the remaining 3N-8 normal modes, treated as harmonic oscillators; note that we use subscript i and j for parameters related to MIN and MAX, respectively. Restricted to the lowest-order coupling terms allowed by symmetry, the iMDH used here thus takes the form

$$\mathcal{H} = -\frac{\hbar^2}{2}\frac{\partial^2}{\partial x^2} - \frac{\hbar^2}{2}\sum_{j=a,s}\frac{\partial^2}{\partial y_j^2} + V(x,y);$$
$$V(x,y) = V_{\rm ad}(x) + \frac{1}{2}\sum_s \omega_s^2(y_s - C_s x^2/\omega_s^2)^2 + \frac{1}{2}\sum_a \omega_a^2(y_a - C_a x/\omega_a^2)^2. \quad (1)$$

Here $V_{\rm ad}(x)$ is the adiabatic potential that connects the two minima at $x = \pm\Delta x$, which is represented by an analytical quartic function, found reliable for proton-transfer processes:[14,15]

$$V_{\rm ad}(x) = V_{\rm ad}(0)[1 - (x/\Delta x)^2]^2. \quad (2)$$

The running subscripts s and a in Eq. (1) indicate modes that are, respectively, symmetric and antisymmetric with respect to reflection in the plane $x = 0$, i.e., modes that are displaced between MIN and MAX, the coupling constants being proportional to the displacements:

$$C_s = \omega_s^2 \Delta y_s/\Delta x^2; \quad C_a = \omega_a^2 \Delta y_a/\Delta x. \quad (3)$$

Although Hamiltonian (1) does not explicitly contain higher-order coupling terms proportional to xy_j^2, $x^2y_j^2$, etc., their effect is partially accounted for by renormalizing the linear coupling constants $C_{a,s}$. Details on the generation of iMDH can be found in Refs. 14, 15, and 18.

Such a Hamiltonian can be generated from electronic-structure and force-field data of MIN and MAX configurations with the antisymmetric imaginary mode $x_{cis} \equiv x_a$ defined by Eq. (A2) "frozen" at zero. Note that the Hamiltonian thus constructed is already of reduced dimensionality, since only modes that are displaced between the stationary points MIN and MAX contribute. Thus of the 106 normal modes y_j at MAX (not counting the imaginary modes), 70 are not displaced and thus do not contribute, leaving only 19 symmetric and 17 antisymmetric modes with coordinates y_s and y_a, respectively. In Table I, we list the relevant modes of each type that are substantially coupled to the tunneling. Since they are still far too numerous to make diagonalization a viable approach, we reduce the dimensionality further by treating weakly coupled modes indirectly through the rescaling of specific parameters. The strength of coupling is measured by the dimensionless parameters $B_{a,s}$, related to the dimensionless

TABLE I. Calculated parameters of the imaginary-mode Hamiltonian (1) for tunneling along the concerted path *trans*-MAX-*trans* in porphycene-d_0/-d_1/-d_2. Frequencies ω_j (at MAX) are in cm^{-1}; the other parameters, viz., coupling constants γ_j, parameters B_j, and zeta-factors ζ_j, defined in Eqs. (4) and (5), are dimensionless. The barrier heights are 4.08 (adiabatic) and 8.76 (crude-adiabatic) kcal/mol; the (mass-weighted) barrier halfwidth Δx = 0.495/0.595/0.675 Å $amu^{1/2}$ and the scaling frequency Ω = 649/540/476 cm^{-1}, respectively. Only modes with $B_j \geq 0.01$ for one of the isotopomers are listed. Modes in bold face are included explicitly in the diagonalization procedure. Parameters are evaluated at the RI-CC2/cc-pVTZ level of theory.

j	ω_j	γ_j	B_j	ζ_j
s modes (a_g)				
13	275/ 274/ 273	0.26/0.32/0.36	0.18/0.21/0.20	0.6/0.7/0.8
17	358/ 358/ 357	0.12/0.17/0.20	0.03/0.03/0.03	0.8/1.0/1.1
18	370/ 369/ 369	0.21/0.26/0.28	0.07/0.07/0.07	0.8/1.0/1.1
33	675/ 672/ 670	0.13/0.17/0.20	0.01/0.01/0.01	1.5/1.8/2.1
56	1031/1031/1031	0.41/0.51/0.55	0.03/0.04/0.03	2.3/2.8/3.2
61	1090/1090/1087	0.36/0.41/0.40	0.02/0.02/0.02	2.5/2.9/3.3
74	1342/1345/1348	0.51/0.50/0.40	0.03/0.02/0.01	3.0/3.6/4.1
90	1592/1597/1435	0.34/0.27/0.60	0.01/0.00/0.02	3.6/4.3/4.4
93	1770/1748/1632	0.84/0.79/0.18	0.05/0.03/0.00	4.0/4.7/5.0
a modes (b_{3g})				
8	145/ 145/ 145	0.04/0.05/0.06	0.02/0.02/0.02	0.3/0.4/0.4
25	608/ 608/ 608	0.16/0.19/0.20	0.01/0.02/0.01	1.4/1.6/1.9
50	896/ 827/ 866	0.27/0.11/0.00	0.02/0.00/0.00	2.0/2.4/2.7
57	1033/1030/1029	0.28/0.29/0.31	0.02/0.01/0.01	2.3/2.8/3.2
59	1080/1078/1076	0.34/0.35/0.33	0.02/0.02/0.00	2.4/2.9/3.9
72	1277/1276/1275	0.11/0.09/0.06	0.00/0.00/0.00	2.9/3.4/3.9
75	1363/1362/1362	0.05/0.09/0.12	0.00/0.00/0.01	3.1/3.6/4.2

coupling constants $\gamma_{s,a}$, both listed in Table I and given by

$$B_{a,s} = \gamma_{a,s}/2\omega_{a,s}^2; \quad \gamma_a = (C_s/\Omega^2); \quad \gamma_s = (C_s/\Omega^2)\Delta x, \tag{4}$$

where the scaling frequency Ω is defined by $\Omega^2\Delta x^2 = V_0$, V_0 being the crude-adiabatic barrier height (which is equivalent to the potential along the linear reaction path).[14,15,18] This "elimination" of weakly displaced modes is possible if their motion is fast on the time scale of tunneling t^* in $V_{\rm ad}(x)$; the latter property is expressed by the condition that the zeta factor

$$\zeta_j = \omega_j t^* \tag{5}$$

be large compared to unity. From previous studies,[14,15] we know that the condition $\zeta_j > 1$ is usually sufficient. In the quasiclassical instanton formalism such modes (marked below by a prime) are treated in the adiabatic approximation.[19,20] This is equivalent to letting the potential in Eq. (1) "relax" over such modes, leading to $y_{a'} = (C_{a'}/\omega_{a'}^2)x$; $\dot{y}_{a'} = (C_{a'}/\omega_{a'}^2)\dot{x}$ and $y_{s'} = (C_{s'}/\omega_{s'}^2)x^2$; $\dot{y}_{s'} = 2x(C_{s'}/\omega_{s'}^2)\dot{x}$, which thus "eliminates" them from the dynamics, but introduces an effective (coordinate-dependent) mass in the quasiclassical kinetic energy operator in the form $\mathcal{T}_m = \frac{1}{2}m(x)\,\dot{x}^2$:

$$m(x) = 1 + a + bx^2; \quad a = \sum_{a'} C_{a'}^2/\omega_{a'}^4; \quad b = 4\sum_{s'} C_{s'}^2/\omega_{s'}^4. \tag{6}$$

Upon quantization,[18] the general Hermitian form of this kinetic energy operator is given by the von Roos Hamiltonian[32]

$$\mathcal{T}_m = \frac{1}{4}(m^\alpha \hat{p}\, m^\beta \hat{p}\, m^\gamma + m^\gamma \hat{p}\, m^\beta \hat{p}\, m^\alpha); \quad \alpha + \beta + \gamma = -1, \tag{7}$$

where $m \equiv m(x)$ and $\hat{p} = -i\hbar\partial/\partial x$ is the momentum operator. It represents a two-parameter family of operators which in general may lead to different results. For this reason it was asserted in Ref. 32 that the effective mass approach is not suitable. However, it has been shown that, in the two-parameter family of Hermitian operators, there is a unique form which is compatible with the additional conditions of Galilean invariance and probabilistic interpretation of the wave function.[33–35] It is given by the symmetric form

$$\mathcal{T}_m = \hat{p}\frac{1}{2m(x)}\hat{p}. \tag{8}$$

This uniqueness of choice allows us to construct a Hamiltonian of reduced dimensionality with $\mathcal{T}_m(x)$, which can be directly diagonalized, and to relate calculated tunneling splittings to observables. In our previous study this approach was adopted for the evaluation of zero-point and mode-specific tunneling splitting in the two isotopomers in malonaldehyde.[18] Here we apply the same approach to the evaluation of tunneling splittings in porphycene.

As seen from the zeta-factors in Table I, most of the coupled modes in porphycene are fast, so that the effect of their coupling can be accounted for collectively through their contribution to the mass-renormalization parameters *a,b* in Eq. (6). This eliminates all but three symmetric modes and one antisymmetric mode from the diagonalization. To diagonalize the resulting Hamiltonian, we previously used a basis set of products $\phi(x)\prod_j \chi(y_j)$, where $\phi(x)$ and $\chi(y_j)$ are harmonic-oscillator eigenfunctions. While the matrix elements of the potential terms with such functions are straightforward, those of the kinetic energy operator (8) require a large number of functions $\phi(x)$ before convergence is achieved, since there are no evident selection rules. Nevertheless, the matrix generated over such a basis is rather sparse and therefore amenable to a modified Jacobi-Davidson algorithm implemented in the Jadamilu software for sparse matrices,[21] tested and applied in our previous study of malonaldehyde.[18] The Hamiltonian to be diagonalized thus contains the *trans* tunneling mode, an antisymmetric mode and (up to) three symmetric modes; for convenience we rewrite it in dimensionless form by expressing energies in units V_0 (the height of the crude-adiabatic potential); coordinates in units Δx; and frequencies and time in units of the scaling frequency Ω, defined above. This leads to a Hamiltonian of the form

$$\begin{aligned}
\mathcal{H}_{5D} &= \mathcal{H}_{1D}(x) + \mathcal{H}_a(y_a) + \sum_{s=1}^{3}\mathcal{H}_s(y_s);\\
\mathcal{H}_{1D} &= -g^2\frac{\partial}{\partial x}\frac{1}{m(x)}\frac{\partial}{\partial x} + (1-B)(1-x^2)^2;\\
\mathcal{H}_s(y_s) &= -g^2\frac{\partial^2}{\partial y_s^2} + \frac{1}{2}\omega_s^2\left(y_s - \frac{\gamma_s}{\omega_s^2}x^2\right)^2,\\
\mathcal{H}_a(y_a) &= -g^2\frac{\partial^2}{\partial y_a^2} + \frac{1}{2}\omega_a^2\left(y_a - \frac{\gamma_a}{\omega_a^2}x\right)^2,
\end{aligned} \tag{9}$$

where $g = \hbar/\Delta x\sqrt{2V_0}$ and $B = \sum_{a,s}B_{a,s}$. In these units, the coordinate-dependent mass in Eq. (6) is given by $m(x) = 1 + \Delta m_{\rm a} + \Delta m_{\rm s}x^2$, where $\Delta m_{\rm s} = 4\sum_{s'}\gamma_{s'}^2/\omega_{s'}^4$, $\Delta m_{\rm a} = \sum_{a'}\gamma_{a'}^2/\omega_{a'}^4$. The characteristic time of motion in the adiabatic potential is $1/\sqrt{1-B}$, so that the parameters $\zeta_{a,s}$ in Eq. (5) used to classify the modes, are given by $\zeta_{a,s} = \omega_{a,s}/\sqrt{1-B}$. The mode parameters are listed in Table I.

To generate the matrix for diagonalization we use as a basis set the combination of the functions $\phi(x)$ and $\chi(y_{a,s})$, mentioned above, which are the eigenfunctions of the zero-order Hamiltonians

$$\begin{aligned}
\mathcal{H}_0 &= g^2\left(-\frac{\partial^2}{\partial x^2} + x^2\right);\\
\mathcal{H}_{a,s}^0(y_{a,s}) &= -g^2\frac{\partial^2}{\partial y_{a,s}^2} + \frac{1}{2}\omega_{a,s}^2 y_{a,s}^2,
\end{aligned} \tag{10}$$

respectively. The antisymmetric and symmetric modes included in the diagonalization are listed in bold in Table I for porphycene and two isotopomers; they are the lowest-frequency observed modes, namely, the antisymmetric mode $a = 8$ and the three symmetric modes $s = 13$, $s = 17$, and $s = 18$. Deuteration of one or both of the mobile protons reduces the splittings to values that, with one exception, have not been resolved to date. This reduction, due to the larger mass of the deuteron, also affects the couplings and, in the case of the HD isotopomer, the kinetic part of the Hamiltonian, as detailed in CDPT; however, since the motion along x_a is "frozen," the kinetic part remains unchanged. Modes $a = 8$ and $s = 13$ are characterized by

TABLE II. Calculated and assigned energy levels and tunneling splittings in porphycene-d_0,-d_1, and -d_2. Energies $E_k^{\pm}$ and frequencies $\omega_{i/j}$ (in Column 5) in cm^{-1}. The two calculated splittings in Column 6 refer to diagonalization results and AIM/DOIT results, respectively, and the observed splittings in Column 7 are taken from Ref. 8.

k	E_k^+	E_k^-	$E_k^+ - E_0^+$	Assignment	ΔE_k^{cal}	ΔE_k^{obs}
Porphycene-d_0						
0	1043.6	1047.7	0	...	4.1/3.8	4.4
1	1188.3	1190.0	145	$\omega_{6/8} = 139/145$	1.7/2.5	<1
2	1263.0	1273.3	219	$\omega_{9/13} = 195/275$	10.3/7.6	12
3	1331.1	1334.5	287	$2 \times \omega_{6/8} = 278/290$	3.4/-	...
4	1393.5	1398.1	350	$\omega_{15/17} = 337/358$	4.4/5.2	4.6
5	1409.3	1413.8	366	$\omega_{16/18} = 363/370$	4.5/5.0	4.6
6	1474.6	1477.7	431	$3 \times \omega_{6/8} = 417$	3.1/-	...
7	1496.2	1517.8	453	$\omega_{9/13} = 390/550$	21.6/24	20
Porphycene-d_1						
0	846.4	846.9	0	...	0.5/1.4	0.58[a]
1	990.0	990.4	144	$\omega_{6/8} = 139/145$	0.5	...
2	1076.1	1078.1	230	$\omega_{9/13} = 195/275$	2.0	2.3
3	1133.5	1134.0	287	$2 \times \omega_{6/8} = 278/290$	0.5	...
4	1201.0	1201.6	355	$\omega_{15/17} = 337/358$	0.6	...
5	1220.0	1221.7	374	$\omega_{16/18} = 363/370$	1.6	...
6	1277.4	1277.6	431	$3 \times \omega_{6/8} = 417$	0.2	...
7	1329.9	1336.5	484	$\omega_{9/13} = 390/550$	6.6	...
Porphycene-d_2						
0	713.9	713.9	0	...	<0.1/0.4	< 0.1[a]
1	857.5	857.6	144	$\omega_{6/8} = 139/145$	≤ 0.1	...
2	941.8	942.2	228	$\omega_{9/13} = 195/275$	0.4	...
3	1001.1	1001.2	287	$2 \times \omega_{6/8} = 278/290$	<0.1	...
4	1085.5	1085.9	372	$\omega_{15/17} = 337/358$	0.3	...
5	1144.8	1144.8	431	$3 \times \omega_{6/8} = 417$	<0.1	...
6	1187.7	1189.2	474	$\omega_{9/13} = 390/550$	1.4	...
7	1229.3	1229.6	515	$\omega_{9/13} = 390/550$	0.4	...

[a]Estimated, Ref. 8.

$\zeta < 1$ and are therefore included in the diagonalization for all isotopomers; the remaining two symmetric modes $s = 17$ and $s = 18$ are treated according to their time scale which depends on the isotopomer. For porphycene-d_0, where concerted tunneling implies a double proton mass, renormalized here to $m(x)$ with a substantial position-dependence, these modes are characterized by $\zeta < 1$ and are therefore included explicitly in the diagonalization; this requires 100 basis functions for x and 10 basis functions for each of the coupled oscillators. For porphycene-d_2, concerted tunneling of a quadruple proton mass requires 200 basis functions for x, so that 5D diagonalization is not feasible; the problem is therefore reduced to 3D, with the modes $s = 17$ and $s = 18$ treated in the adiabatic approximation, as justified by their zeta-factors $\zeta > 1$. The mixed isotopomer porphycene-d_1, where concerted tunneling requires a triple mass, is an intermediate case with zeta-factors $\zeta_{17} \simeq \zeta_{18} \simeq 1$; since it requires 150 basis functions for x, only the stronger-coupled mode $s = 18$ can be explicitly included in the diagonalization, while $s = 17$ is accounted for through mass-renormalization. In Eq. (9) the Hamiltonian is in units V_0=8.76 kcal/mol (the height of the crude-adiabatic potential); the collective parameter $B = 0.53$; the mass-renormalization parameters are $\Delta m_s = 0.37/0.85/1.49$ and $\Delta m_a = 0.08/0.05/0.03$, and $g^2 = 0.0225/0.0155/0.0121$ for porphycene-d_0/-d_1/-d_2, respectively. The respective 5D/4D/3D Hamiltonians are then diagonalized; the eigenvalues of the lowest eight doublets and the corresponding tunneling splittings are listed in Table II. We note that the calculated eigenvalues are not the real energy levels of porphycene, but those of a specially designed imaginary-mode Hamiltonian, where the motion along the x_{cis} coordinate is "frozen"; therefore the lowest energy level cannot be interpreted as zero-point energy.

Table II also lists the tunneling splittings obtained with the AIM/DOIT approach.[22,23] It is based on the Hamiltonian (1) for concerted tunneling which includes *all* the (linearly) coupled skeletal modes listed in Table I.

V. TUNNELING SPLITTINGS AND ASSIGNMENT

As mentioned in the Introduction, Waluk and coworkers[3–5] have measured the tunneling splitting for the zero-point level and several modes assigned as totally symmetric and combinations thereof in emission spectra of porphycene-d_0. Since there are 108 normal modes in porphycene, assigning the five observed modes is not a trivial matter. To achieve a proper assignment, we use the procedure of Ref. 10 and calculated the Dushinsky (**G**-)matrix between the normal modes of the MIN and MAX configurations. The result is shown in Table III, which contains only the parts relevant to the present data and method. A more extensive list is provided in the supplementary material.[29] Waluk *et al.*[8] assumed that the five

TABLE III. Abbreviated list of calculated normal modes of porphycene, labeled i in the MIN and j in the MAX configuration, together with the dominant two **G**-matrix elements that relate them. Frequencies ω are in cm^{-1}. Column 7 indicates pairwise mixing of the numbered modes of the MIN configuration during tunneling.

i/sym	ω_i	j/sym	ω_j	$c_{i,j}$	$c_{i,j'}$	i/i'
4/b_g	108	6/b_{2g}	112	$c_{4,6}=0.99$	$c_{4,7}=0.17$	...
5/b_g	124	7/b_{1g}	136	$c_{5,7}=-0.97$	$c_{5,6}=0.16$	...
6/a_g	139	8/b_{3g}	145	$c_{6,8}=-1.00$	...	...
7/b_g	183	9/b_{1g}	184	$c_{7,9}=0.95$	$c_{7,11}=-0.28$	7/10
9/a_g	195	13/a_g	275	$c_{9,13}=0.92$	$c_{9,18}=0.29$	9/15
10/b_g	196	11/b_{2g}	196	$c_{10,11}=0.96$	$c_{10,9}=0.29$	10/7
12/a_u	288	14/a_u	288	$c_{12,14}=0.97$	$c_{12,15}=-0.26$	12/13
13/a_u	303	15/b_{3u}	301	$c_{13,15}=-0.97$	$c_{13,14}=-0.26$	13/12
15/a_g	337	17/a_g	358	$c_{15,17}=0.70$	$c_{15,18}=-0.62$	15/16
16/a_g	363	18/a_g	370	$c_{16,18}=0.73$	$c_{16,17}=0.68$	16/15
22/a_g	476	23/b_{3g}	480	$c_{22,23}=1.00$	...	...
23/a_g	597	25/b_{3g}	608	$c_{23,25}=-0.98$	$c_{23,1}=-0.15$	...
29/a_u	656	31/b_{3u}	659	$c_{29,31}=0.95$	$c_{29,30}=0.12$	...
30/a_g	662	33/a_g	675	$c_{30,33}=0.99$	$c_{30,1}=0.08$	...
32/b_g	666	32/b_{2g}	665	$c_{32,32}=0.85$	$c_{32,34}=-0.47$	32/33
33/b_g	675	34/b_{1g}	675	$c_{33,34}=-0.88$	$c_{33,32}=-0.48$	33/32
95/a_g	2662	1/b_{3g}	1024i	$c_{95,1}=0.78$	$c_{95,94}=-0.45$	95/92

observed modes are all totally symmetric, since they showed up in an emission spectrum. However, as shown recently for malonaldehyde,[13] for a molecule with a symmetric double-minimum potential leading to tunneling splitting, the symmetry governing the tunneling splitting is not the point group symmetry at the equilibrium configuration, which is C_{2h} in porphycene, but the point group D_{2h} at MAX. Thus the splitting of mode 6 (a_g) at 139 cm^{-1} in MIN is governed by the corresponding mode 8 (b_{3g}) in MAX, which is antisymmetric and should therefore, according to the selection rules,[10] have a splitting equal or smaller than the zero-point splitting, as is indeed observed. Mode 9 at 195 cm^{-1}, an a_g mode which corresponds to the symmetric stretching of the hydrogen bridge, derives its enhanced splitting from its substantial displacement between MIN and MAX. Modes 15 and 16 at 337 and 363 cm^{-1} at MIN, respectively, are both a_g, weakly displaced, and coupled to each other, which qualitatively explains their splitting, which is slightly larger than the zero-point splitting. As detailed in Sec. IV, the mode displacements, to which the corresponding coupling constants are proportional, define the effect on the tunneling splitting.

These observations need to be related to the calculated splittings. The calculated eight split levels of porphycene-d_0, numbered 0–7 in Table II, represent the zero-point level, $E_0^{\pm}$, and seven excited levels of the modes explicitly included in the Hamiltonian. These modes are all totally symmetric in the *trans* configuration MIN, but mode 6 is antisymmetric at MAX, the configuration which determines the frequencies ω_j of the modes in our Hamiltonian. Hence the energy levels cannot be expected to coincide precisely with the calculated frequencies ω_i; we therefore list in Table III also the frequency of the corresponding j mode. The levels $E_1^{\pm}$ are readily assigned to the fundamental of mode $i=6(j=8)$; the fact that it is symmetric in MIN but antisymmetric in MAX explains its reduced splitting relative to the zero-point level.[13] Similarly, the levels $E_2^{\pm}$ are assigned to the fundamental of mode $i=9(j=13)$ which is symmetric in both MIN and MAX. This is the strongly displaced hydrogen-bridge mode, which accounts for its large splitting. To assign the levels $E_4^{\pm}$ and $E_5^{\pm}$, we have to take into account that the modes $i=15(j=17)$ and $i=16(j=18)$ interchange during the transition, as follows from Table III, which means that they combine to form one displaced and one undisplaced local mode.[13] We therefore assign level $E_4^{\pm}$ to the combination ($i=6$ plus $i=9$) and level $E_5^{\pm}$ to the local mode $i=(15+16)/2$. The calculated levels $E_3^{\pm}$ and $E_6^{\pm}$ are assigned to overtones of modes $i=6(j=8)$ and $i=9(j=13)$, respectively. The former is the symmetric overtone of an antisymmetric mode, which rationalizes its larger splitting relative to the fundamental. The large splitting of the overtone of the latter mode is in line with its strong coupling. Higher levels, up to an energy of 1800 cm^{-1} can all be assigned to overtones and combinations of these four modes, but because of the increasing level density at higher energies, these assignments are not always unambiguous.

Thus far our assignments agree with those of Waluk *et al.* However, we have a problem with their assignment of the next fundamental, which they interpreted as an a_g mode with a calculated frequency of 654 cm^{-1} at MIN; it corresponds to mode 30 with a frequency of 662 cm^{-1} in our calculation, according to which it correlates with mode 33 in MAX, where it remains totally symmetric (a_g). Since this fundamental shows no resolvable splitting, this assignment violates the selection rule for symmetric modes;[13] these rules indicate an antisymmetric assignment in MAX corresponding to b_{3g}, whereas the intensity observed in the emission spectrum favors an a_g in MIN. The only available mode of the type is mode 23 in MIN, but its calculated frequency of 597 cm^{-1} in MIN is well below the observed value. Since the selection rules for vibrational tunneling splitting do not extend to combinations and overtones, we leave this problem unresolved.

In principle, one can carry out similar calculations for the *cis* conformer by freezing the motion along the x_s tunneling coordinate, but these levels will be short-lived and have not been observed to date. Of more immediate interest is the splitting in porphycene isotopomers in which one or two of the mobile protons are replaced by deuterons. Using the input data of Table I, we have calculated corresponding level splitting for the two deuterated compounds. Thus far the only measured level splitting is for the levels $E_2^{\pm}$ in porphycene-d_1, which amounts to 2.3 cm^{-1}; our calculated value, reported in Table II, equals 2.0 cm^{-1}. Hence the observed and calculated kinetic isotope effects for this level are the same, namely, according to the data listed for mode 9 in Table II: 12/2.3 = 10.3/2.0 = 5.2. Our calculated zero-point splitting of 0.5 cm^{-1} is below the detection limit of $\simeq 1$ cm^{-1} reported in Ref. 5. We caution, however, that the point group symmetry at MAX is lowered to C_{2h} in this isotomer; the introduced asymmetry may not affect the hydrogen-bridge mode 9 very much, but it is likely to have a strong effect on the splitting of mode 6. The calculations for porphycene-d_2, also reported in Table II, yield zero-point splittings of the order 0.1 cm^{-1}, well below the experimental resolution.

Table II shows reasonably good agreement between the splittings obtained by diagonalization and by the AIM/DOIT approach, which is not surprising, since both methods are based on the same Hamiltonian (1) of concerted tunneling. The agreement is less satisfactory for the two deuterated compounds, and one reason may be the fact that the **G**-matrix used in the AIM/DOIT approach is not fully orthogonal, especially for the mixed isotopomer.

VI. CONCLUSION

The diagonalization method based on a multidimensional imaginary-mode Hamiltonian used here gives a satisfactory account of the observed level splittings in porphycene, its dependence on the specific mode that is excited and its isotope effect, as far as observed. It also produces results that are comparable and indeed slightly superior to those obtained with the approximate instanton method applied to the same Hamiltonian. This Hamiltonian is based on structure and force-field calculations at stationary configurations only, which obviates the need for laborious calculations of a series of intermediate configurations. The results also provide a test for the symmetry selection rules previously derived for excited-level splittings, which predict levels that show no splitting to correspond to antisymmetric modes in the transition state and levels that show an enhanced or equal splitting relative to the zero-point level to correspond to symmetric fundamentals with, respectively, strong and weak coupling to the tunneling mode.

These results obtain a more general significance from the fact that porphycene represents a double-proton transfer system of unusual complexity. Its PES exhibits four minima of two different types, as well as first- and second-order saddle points. Moreover, the energy difference between the minima and their separation by low barriers indicate the possibility of a wide variety of tunneling trajectories, including many that cross classically allowed regions of the PES. In porphycene such crossings are calculated even for the zero-point level. However, if the tunneling protons are correlated, the trajectories are subject to restrictions imposed by the symmetry of the molecule; specifically, the tunneling trajectories correspond, just as normal modes, to the representations of the molecular point group of the second-order saddle point. For porphycene this means that the zero-point tunneling corresponds to concerted double-proton transfer between the two *trans* configurations along a "straight" path. The calculations show that this assumption yields the correct splittings for the zero-point level and the vibrational fundamentals derived from it. The calculations also predict that there will be a corresponding *cis–cis* path at higher energy, but in a molecule as complex as porphycene the corresponding levels will tend to mix with vibrationally excited *trans* levels of the same symmetry and may not be directly observable. Higher-energy levels situated above the barrier will loose their localized character and mix irretrievably with the vibrational manifolds of lower levels.

Although the numerical accuracy of the calculated splittings is very satisfactory, we believe that the main result of this study is the detailed analysis of the effect of proton-proton correlation on the tunneling dynamics and the role of symmetry, an analysis substantiated by the introduction of a new method to solve multidimensional Hamiltonians. These results do not depend on the exact values of the parameters governing the potential energy surface.

APPENDIX: ZERO-POINT SPLITTING IS DUE TO CONCERTED TUNNELING

Here we present details on the symmetry argument of Sec. II of the main text to prove that the zero-point splitting in porphycene is due to concerted tunneling. To achieve that, we use a model 2D Hamiltonian of the same symmetry as the porphycene molecule, which we generate from the calculated data of Sec. III and then diagonalize numerically.

In this model, developed in CDPT, two correlated protons are described by coupled quartic potentials and the Hamiltonian is of the form:

$$\mathcal{H}_{2D} = U_0\left[-\frac{\hbar^2}{U_0\Delta x_0^2}\left(\frac{1}{2m_1}\frac{\partial^2}{\partial x_1^2}+\frac{1}{2m_2}\frac{\partial^2}{\partial x_2^2}\right)\right.$$
$$\left.+(x_1^2-1)^2+(x_2^2-1)^2-4Gx_1x_2\right]. \quad \text{(A1)}$$

Here $m_{1,2}$ are the corresponding masses; $x_{1,2}$ are the dimensionless protons coordinates, in units Δx_0 (half the width of the uncoupled potential); energy is in units U_0 (the barrier height of this potential) and G is the dimensionless parameter of proton-proton correlation. The 2D potentials generated by Eq. (A1) are illustrated in Fig. 2 of CDPT for $G \ll 1$, $0.5 < G < 1$, and $G \gg 1$, respectively; porphycene, with $G = 0.19$ belongs to the first category. The parameters at the stationary points of the potential, expressed as functions of G, are listed in Table I of CDPT.

The representation in individual proton coordinates is useful only when the proton-proton correlation represented by G is smaller than the interaction causing tunneling, which is rarely the case. For porphycene, both the calculated *cis–trans* energy difference and the geometric H/D isotope effect[36] indicate that the protons move concertedly. The two correlated protons are therefore described in terms of the collective parameters

$$x_{s,a} = (x_1 \pm x_2)/2, m_s = m_1 + m_2, \quad \text{(A2)}$$

illustrated in Fig. 4. In this representation, the *trans* configurations (MIN) are at $x_a = 0$, $x_s = \pm\sqrt{1+G}$, with energy zero; the second-order saddle point (MAX) is at the center $x_s = x_a = 0$, with energy $2U_0(1+G)^2$; the *cis* configurations (INT) are at $x_s = 0$, $x_a = \pm\sqrt{1-G}$, with energy $8GU_0$, and there are four transition states (TS) between *trans* and *cis* at $|x_a| = \sqrt{1+2G}/2$, $|x_s| = \sqrt{1-2G}/2$, with energy $U_0(1+2G)^2$. In the case of two protons with mass m_0, $\mathcal{H}_{2D}$ describes concerted motion with mass $m_s = 2m_0$:

$$\mathcal{H}_{2D} = 2U_0\left\{-g^2\left(\frac{\partial^2}{\partial x_s^2}+\frac{\partial^2}{\partial x_a^2}\right)+[x_s^2-(1+G)]^2\right.$$
$$\left.+[x_a^2-(1-G)]^2+6x_s^2x_a^2\right\}, \quad \text{(A3)}$$

where $g = \hbar/2\Delta x_0\sqrt{m_sU_0}$ is a dimensionless parameter.

Equations (A1) and (A3) represent the lowest-order Hamiltonian for two correlated protons, that, for every value

of the correlation strength G, exhibits the proper characteristics of double-proton transfer; at $G < 0.5$ it represents systems with a stable intermediate such as porphycene. Although this Hamiltonian does not include skeletal vibrations and thus is of low dimensionality, its symmetry is the same as that of the porphycene molecule; namely, MAX belongs to the point group D_{2h}, and MIN and INT to the point groups C_{2h} and C_{2v}, corresponding to the *trans* and *cis* configurations, respectively. Therefore, the symmetry arguments of Sec. II apply and the x_s and x_a are separable if the proton-proton correlation is large compared to the tunneling interaction, in which case the protons necessarily move concertedly.

To illustrate the trajectory of the moving protons, we calculate their wave functions (WFs); we proceed in two steps and start with a qualitative analysis. Since each proton moves in a double-minimum potential, its lowest-energy wave function will be a doublet with components denoted by superscripts − and + depending on whether or not they have a node at MAX. Using the two doublets as a lowest-order basis set, we obtain the corresponding WFs of the coupled proton pair by diagonalizing the 4×4 Hamiltonian matrix, which can be done analytically. This yields four eigenvalues, which form doublets $E^{\pm}_{0,1}$, where the lowest eigenvalue E^{+}_{0} corresponds to a WF ϕ^{+}_{0} of symmetry a_g in D_{2h} as well as in C_{2h} and symmetry a_1 in C_{2v}. The second level E^{-}_{0} corresponds to a WF ϕ^{-}_{0} of b_{3g} symmetry in D_{2h}, so that the first doublet ϕ_0 corresponds to concerted double-proton tunneling *trans*-MAX-*trans* between the two *trans* configurations of symmetry a_g in C_{2h}. The order of the other levels and the character of their WFs depend on the magnitude of the correlation factor G and the parameters U_0 and Δx_0. In porphycene, the energy difference between INT and MIN is much larger than the tunneling splitting in each of the uncoupled potentials. Proton motion along the tunneling coordinates belongs to either the b_{3g} or the b_{2u} representation of D_{2h}, corresponding to *trans–trans* or *cis–cis* motion, respectively, the former, which corresponds to ϕ_0, having in porphycene the lower energy. Therefore in porphycene the third and fourth level $E^{\pm}_{1}$, which form the doublet $\phi^{\pm}_{1}$, belong to the b_{2u} representation of D_{2h} and are thus associated with transfer between two *cis* configurations.

To confirm this transfer mechanism, we proceed to the second step and diagonalize the Hamiltonian in Eq. (A3) numerically. To make the results comparable to porphycene, in which a number of skeletal modes are coupled to the tunneling modes, we adjust the calculated parameters of porphycene such that the 2D-PES of our model Hamiltonian closely mimics the adiabatic MD-PES of porphycene. These adjustments are not arbitrary but correspond to adding coupling to skeletal modes to the 2D Hamiltonian and treating these modes in the adiabatic approximation. This means that the adjusted 2D Hamiltonian is equivalent to the proper MD porphycene Hamiltonian with all coupled modes treated as fully relaxed. This approximation is not valid for all coupled modes, but is the best available first approximation. This results in $U_0 = 500\ \text{cm}^{-1}$, $\Delta x_0 = 0.37$ Å, and G = 0.2. With these parameters, the energies of INT, TS, and MAX are 2.29 kcal/mol, 2.80 kcal/mol, and 4.11 kcal/mol, respectively, close to those reported in Fig. 3. The calculated value $\Delta x_0 = 0.32$ Å has been modified to $\Delta x_0 = 0.37$ Å, so that the eigenvalues reported below mimic those from the MD diagonalization of Sec. IV. Note that, since this model Hamiltonian operates with *adiabatic* energy barriers, the zero-point splitting $\Delta E_0 = 35.3\ \text{cm}^{-1}$ resulting from it well exceeds the actual one calculated for the MD Hamiltonian.

The Hamiltonian of Eq. (A3) with these parameters is diagonalized numerically, and the eigenvalues of the two lowest doublets are $E^{+/-}_{0} = 989.3/1024.6\ \text{cm}^{-1}$ and $E^{+/-}_{1} = 1453.4/1493.5\ \text{cm}^{-1}$, with wave functions $\phi^{+/-}_{0}$ and $\phi^{+/-}_{1}$, respectively, illustrated in Fig. 4. Note that, for the current 2D model Hamiltonian, $E_0 >$ INT ($= 800\ \text{cm}^{-1}$); yet, the wave functions $\phi^{+/-}_{0}$, shown in Fig. 4, are localized at MIN with the typical 1D tunneling behavior along the symmetric x_s coordinate as predicted by symmetry. Similarly, $E_1 \geq$ MAX ($= 1440\ \text{cm}^{-1}$), but the wave functions $\phi^{+/-}_{1}$ retain the image of correlated tunneling along the antisymmetric x_a coordinate as again predicted by symmetry. Continuing the calculation to higher levels, situated well above MAX, we find that the correlation is fading in favor of a typical vibrational progression, especially for the levels without a node at MAX. Thus while the symmetric state ϕ^{+}_{2} corresponding to the fifth level ($E_5 = 2442.9\ \text{cm}^{-1}$) is spread almost equally over the two tunneling coordinates, Fig. 4 shows that the sixth, antisymmetric level at energy $E_6 = 3255.6\ \text{cm}^{-1}$ located well above MAX, retains some preference for x_s. Thus the model provides a continuous transition between levels arranged as split pairs and levels arranged as a vibrational progression.

This numerical analysis confirms the conclusion drawn from general symmetry arguments of Sec. II of the main text that the zero-point tunneling splitting in porphycene is due to concerted double-proton tunneling *trans*-MAX-*trans* along x_s with an imaginary frequency $\omega^{*}_{s} = 1024i\ \text{cm}^{-1}$. Therefore, in Sec. IV of the main text we calculate this splitting and that of excited vibrational levels derived from it using a single-particle approach to concerted tunneling and "freezing" the motion associated with the second imaginary frequency $\omega^{*}_{a} = 841i\ \text{cm}^{-1}$ along x_a.

[1] Z. Smedarchina, W. Siebrand, A. Fernández-Ramos, and R. Meana-Pañeda, Z. Phys. Chem. **222**, 1291 (2008).
[2] J. R. Roscioli, D. W. Pratt, Z. Smedarchina, W. Siebrand, and A. Fernández-Ramos, J. Chem. Phys. **120**, 11351 (2004).
[3] Z. Smedarchina, W. Siebrand, and A. Fernández-Ramos, J. Chem. Phys. **127**, 174513 (2007).
[4] R. H. McKenzie, J. Chem. Phys. **141**, 104314 (2014).
[5] E. Vogel, M. Köcher, H. Schmickler, and J. Lex, Angew. Chem., Int. Ed. Engl. **25**, 257 (1986).
[6] J. Sepioł, A. Stepanenko, A. Vdovin, A. Mordzinski, E. Vogel, and J. Waluk, Chem. Phys. Lett. **296**, 549 (1998).
[7] J. Waluk, Acc. Chem. Res. **39**, 945 (2006).
[8] A. Vdovin, J. Waluk, B. Dick, and A. Slenczka, ChemPhysChem **10**, 761 (2009).
[9] K. Malsch and G. Hohlneicher, J. Phys. Chem. A **101**, 8409 (1997).
[10] P. M. Kozlowski, M. Z. Zgierski, and J. Baker, J. Chem. Phys. **109**, 5905 (1998).
[11] M. F. Shibl, M. Tachikawa, and O. Kühn, Phys. Chem. Chem. Phys. **7**, 1368 (2005).
[12] Z. Smedarchina, M. F. Shibl, O. Kühn, and A. Fernández-Ramos, Chem. Phys. Lett. **436**, 314 (2007).
[13] W. Siebrand, Z. Smedarchina, and A. Fernández-Ramos, J. Chem. Phys. **139**, 021101 (2013).

[14]Z. Smedarchina, W. Siebrand, and A. Fernández-Ramos, J. Chem. Phys. **137**, 224105 (2012).
[15]Z. Smedarchina, W. Siebrand, and A. Fernández-Ramos, J. Phys. Chem. A **117**, 11086 (2013).
[16]O. Christiansen, H. Koch, and P. Jørgensen, Chem. Phys. Lett. **243**, 409 (1995).
[17]T. H. Dunning, Jr., J. Chem. Phys. **90**, 1007 (1989).
[18]A. Fernández-Ramos, Z. Smedarchina, and W. Siebrand, Phys. Rev. E **90**, 033306 (2014).
[19]J. P. Sethna, Phys. Rev. B **24**, 698 (1981); **25**, 5050 (1982).
[20]V. A. Benderskii, V. I. Goldanskii, and D. E. Makarov, Chem. Phys. Lett. **171**, 91 (1990); Chem. Phys. **154**, 407 (1991).
[21]M. Bollhöfer and Y. Notay, Comput. Phys. Commun. **177**, 951 (2007).
[22]W. Siebrand, Z. Smedarchina, M. Z. Zgierski, and A. Fernández-Ramos, Int. Rev. Phys. Chem. **18**, 5 (1999); Z. Smedarchina, A. Fernández-Ramos, and W. Siebrand, J. Comput. Chem. **22**, 787 (2001).
[23]Z. Smedarchina, A. Fernández-Ramos, W. Siebrand, and M. Z. Zgierski, DOIT 2.0, a computer program to calculate hydrogen tunneling rate constants and splittings, National Research Council of Canada, 2006.
[24]C. Hättig, J. Chem. Phys. **118**, 7751 (2003).
[25]J. Yang, G. K.-L. Chan, F. R. Manby, M. Schütz, and H.-J. Werner, J. Chem. Phys. **136**, 144105 (2012).
[26]Y. Horbatenko and S. F. Vyboishchikov, ChemPhysChem **12**, 1118 (2011).
[27]L. Wang, M. Ceriotti, and E. Markland, J. Chem. Phys. **141**, 104502 (2014).
[28]TURBOMOLE, version 5.9, University of Karlsruhe and Forschungszentrum Karlsruhe GmbH (2007).
[29]See supplementary material at http://dx.doi.org/10.1063/1.4900717 for the list of the frequencies of the normal modes of porphycene for the stationary point structures, and the **G**-matrix coefficients between the normal modes of MIN and MAX configurations of porphycene.
[30]R. H. McKenzie, C. Bekker, B. Athokpam, and S. G. Ramesh, J. Chem. Phys. **140**, 174508 (2014).
[31]W. W. Cleland, Adv. Phys. Org. Chem. **44**, 1 (2010).
[32]O. von Roos, Phys. Rev. B **27**, 7547 (1983).
[33]P. V. Elyutin and V. D. Krivchenkov, Theor. Math. Phys. **16**, 939 (1973).
[34]I. M. Sokolov, Zh. Eksp. Teor. Fiz. (JETP) **89**, 556 (1985).
[35]J. Thomsen, G. T. Einevoll, and P. C. Hemmer, Phys. Rev. B **39**, 12783 (1989).
[36]M. F. Shibl, M. Pietrzak, H. H. Limbach, and O. Kuhn, ChemPhysChem **8**, 315 (2007).